Supporting Information

Dual Stimuli-Responsive Nanoparticle-Incorporated Hydrogels as an Oral Insulin Carrier for Intestine-Targeted Delivery and Enhanced Paracellular Permeation

Liang Liu,[a,b] Ying Zhang,[a,b] Shuangjiang Yu,[a] Zhiming Yang,[c] Chaoliang He,[a,*] Xuesi Chen[a,*]

[a] Key Laboratory of Polymer Ecomaterials, Changchun Institute of Applied Chemistry, Chinese Academy of Sciences, Changchun 130022, China

[b] University of Chinese Academy of Sciences, Beijing 100039, China

[c] Department of Orthopaedics, The First Hospital of Jilin University, Changchun 130021, China

* Corresponding authors. E-mail addresses: clhe@ciac.ac.cn (C. He); xschen@ciac.ac.cn (X. Chen).

Supplementary Information: Number of pages: 31

Number of figures: 15

Number of tables: 3

Number of illustrations: 2

S1. Supplementary experimental methods.

S1.1. Synthesis of CMS-*g*-AA.

The acrylate-*grafted*-carboxymethyl starch (CMS-*g*-AA) was synthesized *via* a coupling reaction between the hydroxyl of carboxymethyl starch (CMS) and the carboxyl of acrylic acid (AA). Typically, AA (0.20 g) was reacted with EDC·HCl (0.64 g) and DMAP (0.04 g) in 2 mL solvent of DMSO. After activation for 24 h of the carboxyl groups, the AA solution was then added into 30 mL of carboxymethyl starch solution (CMS, 1.0 g, dissolved in PBS) drop by drop. The reaction was allowed to proceed for an additional 48 h at room temperature and was purified by dialysis against DI-water for 3 days, followed by lyophilization. The substitution degree of acrylate groups in CMS-*g*-AA was calculated according to the results of elemental analysis.

S1.2. Preparation and characterization of CMS-*g*-AA/PMAA hybrid hydrogel.

CMS-*g*-AA/PMAA hybrid hydrogel was prepared *via* the following procedure. Typically, the mixture of CMS-*g*-AA and methacrylic acid (MAA) were dissolved in DI-water. After uniform dispersion, APS and TEMED, serving as the initiator and accelerator, were both added to start the free radical polymerization at the room temperature. The gelation reaction was allowed to proceed under nitrogen protection for 24 hours. The feed ratios of the monomer and other reactants were listed in **Table S1**. Finally, the hydrogel products were transferred into the 200 mL beakers and immersed into DI-water. The DI-water was refreshed frequently for 7 days to remove the impurities, followed by freeze-drying. The compositions of the resulting hydrogel samples were determined according to the results of elemental analysis (**Table S1**).

S1.3. Swelling behavior of CMS-*g*-AA/PMAA hybrid hydrogel.

To investigate the swelling process of the hydrogels, the swelling kinetics tests were performed. Dried cylinder-shaped gel samples (80 – 90 mg) were immersed into 50 mL of normal saline with different pH values of 1.2, 6.0, 6.8 and 7.4, under a shaking rate of 100 rpm at 37 ^{o}C. At distinct time intervals, the swollen samples were taken out for weighing after wiping off the external liquid drops

with the filter paper. Then the samples were immersed again into the swelling media to continue the swelling process. The exterior swelling medium was refreshed every hour. The swelling ratio (SR) of the hydrogel was calculated according to the **Equation S1** below:

$$SR = (W_t - W_0) / W_0 \qquad (S1)$$

where W_t and W_0 are the weights of the swollen gels and the dehydrated samples, respectively.

For further evaluation of the equilibrium swelling ratios (ESRs) of the hydrogels, the swelling process was conducted for 48 h to ensure the achievement of swelling equilibrium in the swelling media with different pH values from 1.0 to 8.0. The tests were carried out in triplicate for average.

S1.4. *In vitro* enzymatic degradation of CMS-*g*-AA/PMAA hybrid hydrogel.

The enzymatic degradation measurements of the hydrogels were carried out to demonstrate the degradable properties under pepsin (800 U/mL) in artificial gastric fluid (AGF), trypsin (3000 U/mL) in artificial intestinal fluid (AIF), and α-amylase (100 U/mL) in AIF, respectively. Typically, dried cylinder-shaped gel samples (40 – 45 mg) were immersed into 25 mL of degradation media with different enzymatic environments, under a shaking rate of 100 rpm at 37 ^{o}C. At distinct time intervals, the hydrogel residues were taken out and rinsed with fresh AGF or AIF thoroughly to get rid of enzyme molecules and the degraded fragments, followed by lyophilization. The weights of dried hydrogel residues after degradation were obtained. The gel weight remaining (GWR, of initial %) was calculated according to the following **Equation S2**:

$$GWR\ (\%) = (W_{dr} / W_{d0}) \times 100 \qquad (S2)$$

where W_{d0} and W_{dr} are the weights of the dried intact hydrogel before enzymatic degradation and the hydrogel residue after enzymatic degradation, respectively. The exterior degradation media were refreshed every hour. All the tests were carried out in triplicate to report the average values.

S1.5. Morphology of CMS-*g*-AA/PMAA hybrid hydrogel.

Morphologies of the hydrogel samples were investigated by the environmental scanning electron microscopy (ESEM) on an XL 30 ESEM FEG Scanning Electron Microscope (Micrion FEI PHILIPS) after incubating the hydrogels in different media.

The hydrogel samples were immersed in AIF to reach the swelling equilibrium. Besides, the dried hydrogel samples were also incubated in AIF with α-amylase (100 U/mL) for 30 min. All the treated samples were immediately put into liquid nitrogen for 10 min, followed by freeze-drying. The resulting specimens were fixed on a copper SEM specimen holder and coated with sputtered gold for observation.

S1.6. Cell culture.

Caco-2 cells (human colon carcinoma, clone 1) were purchased from the Type Culture Collection of the Chinese Academy of Sciences (Shanghai, China). Caco-2 cells were cultivated on cell culture flasks using MEM cell culture medium (Grand Island, N.Y., USA) with 10% fetal bovine serum.

Caco-2 cell monolayer was obtained through the following procedure. Typically, Caco-2 cells were cultured on the polycarbonate filter membrane with a density of 3.0×10^5 cells per well in Costar Transwell 24 well/plates (membrane pore diameter of 0.4 μm, Corning Costar Corp., N.Y.). The cell monolayer was used for experiments approximately 21 days after seeding. To verify the integrity of the cell monolayer, the transepithelial electric resistance (TEER) was measured with an Epithelial Volt-Ohm Meter (Millicell ERS-2 MILLIPORE Corp., USA), and was found to be in the range from 180 to 220 $\Omega \cdot cm^2$.

S1.7. Animal experiments.

Male SD rats (7 to 8 weeks) were induced *via* a single intraperitoneal injection of streptozotocin (STZ, dissolved in 10 mM citrate buffer at pH 4.5) at the STZ dose of 55 mg/kg body weight, as the type-1 diabetic (T1D) animal model. The rats were considered diabetic when their fasting blood glucose levels were over 16.7 mmol/L. During the *in vivo* pharmacodynamics assay, the diabetic rats were remained fasted, but with free access to water.

S1.8. Mucosa affinity of CS/Ins/HS NPs.

CS/Ins/HS NPs were tested for the mucosa affinity *via* the measurements of the particle size and zeta-potential of the nanoparticle-specimens after being incubated in the mucin solution. Typically, CS/Ins/HS NPs were dispersed in DI-water (pH 6.0), followed by blending with the fresh mucin solution. All the mixtures were stirred for 2 h before testing. The final nanoparticle-concentration in different mixtures was set as 1.0 mg/mL, while the final mucin-concentrations in different mixtures were set as 0, 0.01, 0.02, 0.04, 0.08, 0.1, 0.2, 0.4 and 0.8 mg/mL, respectively. Besides, the ionic strength for each sample was controlled to be 0.15 M by adding sodium chloride (NaCl). Both the particle size and zeta-potential for each sample were tested at 37 ^{o}C on a Zeta Potential/BI-90Plus Particle Size Analyzer (Brookhaven, USA).

Moreover, quantitative assay of the mucin adhering onto CS/Ins/HS NPs was carried out with the following procedure. Typically, CS/Ins/HS NPs were dispersed in 10 mL of DI-water (2.0 mg/mL, pH 6.0), and mixed with an equal volume of fresh mucin solution (0.8 mg/mL, pH 6.0). After incubation at 37 ^{o}C for 2 h, the mucin-adhered nanoparticles were collected by centrifugation and were rinsed to remove the dissociative mucin, followed by lyophilization for XPS measurements. Meanwhile, the supernatant was obtained following centrifugation, and was diluted for detection of the dissociative mucin on a UV/Vis spectrophotometer (Shimadzu UV-2401PC). As the control, 10 mL of fresh mucin solution (0.8 mg/mL, pH 6.0) was blended with 10 mL of DI-water, and treated in the same procedure. The mucin adhesion capacity (MAC %) was defined to reflect the potential mucosa affinity of CS/Ins/HS NPs and was calculated according to the **Equation S3** below:

$$MAC(\%)=\frac{(W_{MT}-W_{MS})}{W_{NP}+(W_{MT}-W_{MS})}\times 100 \qquad (S3)$$

where W_{MT} is the total weight of mucin in the fresh mucin solution, W_{MS} is the weight of the dissociative mucin in the supernatant after incubating with the nanoparticle-specimens, and W_{NP} is the weight of the dehydrated CS/Ins/HS NPs for feeding. All the experiments were carried out in triplicate, and the average values were reported.

S1.9. Ca^{2+}-binding capacity of heparin sodium at different pH.

Heparin sodium (HS) was dissolved in DI-water with the concentration of 0.25 mg/mL. Then, 0.25 mL of calcium chloride titrant ($CaCl_2$, 0.5 M) was added into 20 mL of the HS solution, and the pH of the mixture was adjusted from 2.0 to 8.0. After incubating in different pH conditions for 2 h at 37 ^oC, anhydrous ethanol was added for precipitating heparin calcium salt. The dissociative Ca^{2+} ions in the supernatant were collected by centrifugation, and diluted for detection on an inductive coupled plasma emission spectrometer (ICP-OES, iCAP 6300, Thermoscientific, USA). The Ca^{2+}-binding capacity (μg/mg) of heparin sodium was defined as the chelated-calcium weight (unit: μg) divided by the feeding heparin sodium weight (unit: mg). The tests for each sample were carried out in triplicate to present the average result.

S1.10. *In vitro* protease inhibition assay.

In vitro protease inhibition assay was carried out by testing the remaining bioactivity of insulin after incubating the free-form insulin, the Ins/HS aggregates, or the CS/Ins/HS NPs with trypsin for different time periods. Typically, the free-form insulin, the Ins/HS aggregates, and the CS/Ins/HS NPs were all dissolved in AIF (containing 150 U/mL of trypsin), with the insulin concentration of 1.0 mg/mL for each group. Followed, the mixtures were incubated at 37 ^oC under a shaking rate of 100 rpm. At distinct time intervals, the proteolysis was stopped by adding TFA. The insulin residues were collected and diluted in PBS (pH 7.4) for detection of the remaining bioactivity with the porcine insulin ELISA kits. Meanwhile, the fresh insulin without proteolysis was tested in the same procedure, and its remaining bioactivity was regarded as 100%.

S1.11. Effects of CS/Ins/HS NPs on Caco-2 cell monolayer.

Effects of CS/Ins/HS NPs on the integrity of Caco-2 cell monolayer were investigated with the following procedure. Typically, the nanoparticle-specimens were dispersed in DI-water, and the pH was adjusted to pH 6.0, pH 6.8 or pH 7.4. Followed, 100 μL of the sample solution (1.0 mg/mL) was added into the upper compartment of each well, while 600 μL of fresh culture medium was added

into the lower compartment. After incubation for 2 h, the sample solution in the upper compartment was replaced by the fresh culture medium. During the whole experimental process, the changes of transepithelial electric resistance (TEER) for the Caco-2 cell monolayer were monitored at different time intervals. And the free-form insulin solution was set as the negative control. All tests were conducted in quadruplicate for the average results.

Additionally, both the chitosan solution (CS, 1.0 mg/mL) at pH 6.0, 6.8 or 7.4, and the heparin sodium solution (HS, pH 7.4) in different concentrations from 1.0 mg/mL to 20.0 mg/mL, were investigated for the effects on the integrity of Caco-2 cell monolayer.

S1.12. Calcium-depletion by heparin sodium on Caco-2 cells.

To evaluate the calcium levels on Caco-2 cells, the flow cytometer was used to detect the fluorescent intensity of calcein on the calcein-stained cells. Typically, Caco-2 cells were seeded on 12-well plates at 2.0×10^5 cells/well and incubated for 24 h. Then, the cell culture medium was replaced by the heparin sodium solution (HS, pH 7.4) with different HS concentrations from 1.0 mg/mL to 20.0 mg/mL. After 60 min of incubation, the cells were collected and stained with calcein (1 μg/mL). The calcium levels on the dyed Caco-2 cells were determined by testing the fluorescent intensity of calcein with a Guava EasyCyte flow cytometer (Guava Technologies).

For observation of the calcein-stained Ca^{2+}-distribution, Caco-2 cells were grown on cover-slips in 6-well plates at 2.0×10^5 cells/well and incubated for 24 hours before experiments. Followed, the cell culture medium was replaced by the heparin sodium solution (HS, pH 7.4) with different HS concentrations from 1.0 mg/mL to 20.0 mg/mL. After 60 min of incubation, the cells on cover-slips were washed thoroughly with PBS and fixed with 3.7% paraformaldehyde for 15 min at room temperature. The cell nucleus was stained by 4'-6-diamidino-2-phenylindole (DAPI, 1.0 mg/mL, adding 1 μL per well) for 15 min, and the Ca^{2+} ions on the cells were stained by calcein (1 μg/mL) for 30 min, followed by observation on a CLSM (ZEISS LSM780, Germany).

S1.13. Visualization of tight junctions disruption.

The visualization of the disruption of tight junctions (TJs) between the contiguous Caco-2 cells was performed with the following procedure. Typically, Caco-2 cells were seeded on cover-slips in 6-well plates at 4.0×10^5 cells/well and incubated for 72 h to form compact cell layer. The CS/Ins/HS NPs were dispersed in the artificial intestinal fluid (AIF, pH 6.8) as the sample solution with the concentration of 1.0 mg/mL. The obtained compact cell layers were incubated with the sample solution for different time periods (0 min, 15 min, 30 min, 60 min and 120 min). After incubation, the cells on cover-slips were washed thoroughly with PBS to remove the extracellular residues, and fixed with 3.7% paraformaldehyde for 15 min at room temperature. The cell nucleus was stained by 4'-6-diamidino-2-phenylindole (DAPI). The F-actin was stained by Alexa Fluor 488 phalloidin. The ZO-1 was stained by Alexa Fluor 647 ZO-1 monoclonal antibody. The dyed cells were observed by CLSM.

S2. Supplementary results and discussion.

S2.1. Electrostatic interaction in CS/Ins/HS NPs at various pH conditions.

In **Fig. S3**, the reflective FT-IR spectra of CS/Ins/HS NPs were investigated at different pH from 2.0 to 7.0. The characteristic peaks observed at 1724 cm^{-1} (Peak b) and 1385 cm^{-1} (Peak d) were assigned to the protonated carboxyl groups (-COOH) and ionized sulfonic groups (-O-SO_2-O^- and -NH-SO_2-O^-) in heparin sodium. While the peaks at 1638 cm^{-1} (Peak a) and 1537 cm^{-1} (Peak c) belonged to the carbonyl (C=O) of methanamide groups and protonated amino groups (-NH_3^+) in chitosan. Besides, the strong peaks ranging from 1200 cm^{-1} to 1000 cm^{-1} (Region f) could be ascribed to the sulfo groups (S=O) in heparin sodium. Hence, according to the observation in the spectra, the carboxyl groups (Peak b) of heparin sodium were partially protonated below pH 5.0, but were completely ionized when the pH value was above 6.0. The intensity for the peak (Peak d) of the ionized sulfonic groups (-O-SO_2-O^- and -NH-SO_2-O^-) in heparin sodium presented obvious decrease at pH 2.0, indicating that the sulphate monoesters and sulphamido groups were gradually protonated. However, the typical peak (Peak c) of the protonated amino groups (-NH_3^+) in chitosan could be

observed in the whole testing pH range from pH 2.0 to pH 7.0, implying the existence of electrostatic interactions between chitosan and heparin sodium.

S2.2. MALDI-TOF MS analysis of insulin and insulin residues.

MALDI-TOF MS analysis was carried out for the fresh insulin or the insulin residues after incubating with trypsin (150 U/mL) for 60 min, as shown in **Fig. S4**. According to the results in **Fig. S4A** and **Fig. S4B**, the molecular ion peak for fresh insulin disappeared after trypsin-degradation, implying that most of the insulin molecules were degraded into fragments within 60 min. Besides, as compared with the insulin residue collected from the group of Ins/HS aggregates after trypsin-degradation (**Fig. S4C**), the insulin residue collected from the group of CS/Ins/HS NPs exhibited less fragments in the spectrum (**Fig. S4D**), indicating that insulin could be protected against the proteolysis of trypsin after being encapsulated into CS/Ins/HS NPs.

S2.3. Characterization of CMS-*g*-AA/PMAA hybrid hydrogel.

According to the results of elemental analysis, the weight content (wt%) of acrylate group in CMS-*g*-AA was calculated to be 9.4 wt%. By changing the feeding ratios of CMS-*g*-AA and MAA, a series of hydrogels with different compositions were prepared, as shown in **Table S1**.

The FT-IR spectra of CMS, CMS-*g*-AA, Gel-0, Gel-1, Gel-2 and Gel-3 were shown in **Fig. S9**. The typical absorption peak at 1603 cm^{-1} appeared for all the samples, which was attributed to the carbonyl of the carboxymethyl group in CMS. In the spectrum of CMS-*g*-AA, a new absorption peak at 1653 cm^{-1} was observed, which was related to the carbonyl group from AA. This result indicated the successful coupling between AA and CMS *via* the ester bond. Moreover, the characteristic absorption peak at 1733 cm^{-1} was observed in the spectra of Gel-1, Gel-2, and Gel-3, except for Gel-0 (free of PMAA content), which was assigned to the carbonyl group of MAA. With the increasing PMAA content of the hydrogels, the intensity of the absorption peak at 1733 cm^{-1} exhibited a marked increase.

S2.4. pH-sensitivity of CMS-*g*-AA/PMAA hybrid hydrogel.

To evaluate the swelling performance of Gel-2, the swelling kinetics measurements were conducted at different pH, mimicking the gastric pH (pH 1.2) and the intestinal pH (pH 6.0, pH 6.8 and pH 7.4), as shown in **Fig. S10**. It was found that Gel-2 could keep the shrinking state at pH 1.2 for at least 12 h, with an extremely low swelling ratio (SR) of ~5.0. When the pH was increased to above 6.0, the swelling of Gel-2 was accelerated, which was desirable for the pH-triggered release in small intestine. The equilibrium swelling ratios (ESRs) of Gel-2 were measured at different pH from 1.0 to 8.0, as shown in **Fig. S11**. In acidic media below pH 4.0, Gel-2 exhibited low ESRs, due to the protonation of PMAA (pK_a < 5.0) segments in gel-networks. However, with increasing the pH to above 5.0, the ESRs of Gel-2 showed marked increase, due to the thorough ionization of the carboxyl groups in Gel-2. As shown in **Fig. S12**, the swelling of Gel-2 was observed after reaching the swelling equilibrium in AGF or in AIF. In AGF, Gel-2 was shrunken and opaque, presenting a dehydrated state. Conversely, in AIF, Gel-2 was swollen and hyaline, containing an appreciable amount of water inside the gel-networks.

S2.5. Enzymatic degradation of CMS-*g*-AA/PMAA hybrid hydrogel.

The enzymatic degradation of Gel-2 was investigated, as shown in **Fig. S14**. In the gel-networks, the CMS component and PMAA component were linked with each other *via* the ester bond, which could be degraded in strongly acidic environment of stomach. Meanwhile, the hydrolysis of CMS could occur in the acidic condition. Hence, after incubating for 2 h in AGF (containing pepsin, mimicking the gastric environment), Gel-2 showed certain weight loss with 95.7% of GWR. The degradation degree of Gel-2 in AGF was considered to be rather slight under the protection of the acid-proof PMAA component. Moreover, certain weight loss of Gel-2 could also be observed after incubating in AIF (containing trypsin) under a shaking rate of 100 rpm. It should be ascribed to the fact that the drastically decreased physical strength of gel-networks in the swollen state led to the fragmentation and disaggregation of Gel-2. However, more rapid disintegration of Gel-2 occurred under the effect of α-amylase in AIF, due to the enzymatic degradation of the CMS component in the gel-networks.

So the GWR of Gel-2 was 24.5% after incubating for 2 h in AIF with α-amylase. Furthermore, the morphology of Gel-2 was investigated by the environmental scanning electron microscopy (ESEM) after reaching the swelling equilibrium in AIF in absence of α-amylase (**Fig. S13A**) or after being incubated for 30 min in AIF in presence of α-amylase (**Fig. S13B**).

Table S1. Feed ratios and compositions of CMS-*g*-AA/PMAA hybrid hydrogel

Sample codes	Feeding ratios				CMS (wt%)[a]	PMAA (wt%)[b]	Yield (%)[c]	Conversion of MAA (%)
	CMS-*g*-AA [g]	MAA [g]	APS [mg]	TEMED [μL]				
Gel-0	1.0	0	25	25	100%	0%	87%	-
Gel-1	1.0	0.1	25	25	93%	7%	91%	71%
Gel-2	1.0	0.2	25	25	86%	14%	93%	83%
Gel-3	1.0	0.4	25	25	80%	20%	81%	69%

[a)]Weight content of CMS component in dried hydrogels, calculated from elemental analysis results.

[b)]Weight content of PMAA component in dried hydrogels, calculated from elemental analysis results.

[c)]Calculated from the following equation: Yield (%) = $W_H/(W_C + W_M)$, where W_H was the weight of dried hydrogel, W_C was the feeding weight of CMS-*g*-AA and W_M was the feeding weight of MAA.

Table S2. Characterization of the Ins/HS aggregates after assembly

Sample Codes	Ins Solution (mL)	HS Solution (mL)	Ins/HS Ratio (wt/wt)	Particle Size[a] (nm)	Zeta Potential[b] (mV)
Insulin solution	3	-	-	4.3 ± 1.2	7.6 ± 5.1
Ins/HS aggregate-1	3	0.375	4/1	1374.2 ± 32.6	-29.8 ± 1.9
Ins/HS aggregate-2	3	0.75	2/1	295.5 ± 7.7	-34.9 ± 3.4
Ins/HS aggregate-3	3	1.5	1/1	254.2 ± 4.9	-35.4 ± 4.0
Ins/HS aggregate-4	3	3	1/2	248.5 ± 4.4	-43.8 ± 2.5
Ins/HS aggregate-5	3	6	1/4	218.1 ± 5.5	-40.5 ± 3.3
Ins/HS aggregate-6	3	12	1/8	199.6 ± 1.7	-43.3 ± 2.5

[a)]Particle size and [b)]zeta-potential of the fresh insulin solution before assembly and the Ins/HS aggregates after assembly were measured at pH 4.0. Notably, the concentrations of insulin (Ins) and heparin sodium (HS) solutions were 1.0 mg/mL and 2.0 mg/mL, respectively.

Table S3. Characterization of the CS/Ins/HS NPs in various formulations

Sample Codes	Ins Solution (mL)	HS Solution (mL)	Ins/HS Ratio (wt/wt)	CS Solution (mL)	Particle Size (nm)	Zeta Potential (mV)	DLC[a] (%)	EE[b] (%)
CS/Ins/HS NPs-1	3	0.375	4/1	3	634.4 ± 4.8	10.2 ± 4.2	3.9 ± 0.9	3.3 ± 0.8
CS/Ins/HS NPs-2	3	0.75	2/1	6	589.9 ± 4.8	12.5 ± 3.7	7.7 ± 1.7	7.9 ± 2.6
CS/Ins/HS NPs-3	3	1.5	1/1	12	450.2 ± 6.3	19.4 ± 1.9	10.9 ± 0.8	10.0 ± 1.1
CS/Ins/HS NPs-4	3	3	1/2	24	422.9 ± 5.3	17.2 ± 2.2	15.2 ± 1.4	14.2 ± 2.4
CS/Ins/HS NPs-5	3	6	1/4	48	408.4 ± 4.6	22.8 ± 2.9	9.7 ± 1.4	23.5 ± 3.1
CS/Ins/HS NPs-6	3	12	1/8	96	403.0 ± 2.6	29.6 ± 1.6	8.5 ± 1.8	28.1 ± 5.6

[a)]DLC was defined as the drug loading content of insulin, while [b)]EE represented the entrapment efficiency of insulin. Notably, the concentrations of insulin (Ins), heparin sodium (HS) and chitosan (CS) solutions were 1.0 mg/mL, 2.0 mg/mL and 1.5 mg/mL, respectively.

A. Macromolecular Crosslinker CMS-*graft*-AA:

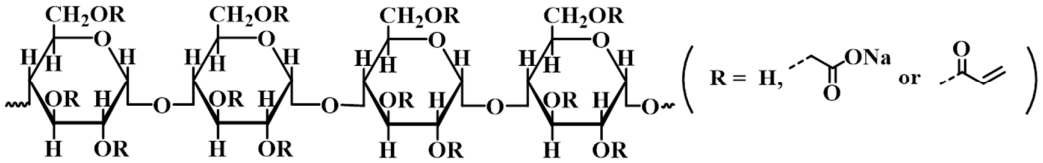

B. Preparation of CMS-*g*-AA/PMAA Hybrid Hydrogel:

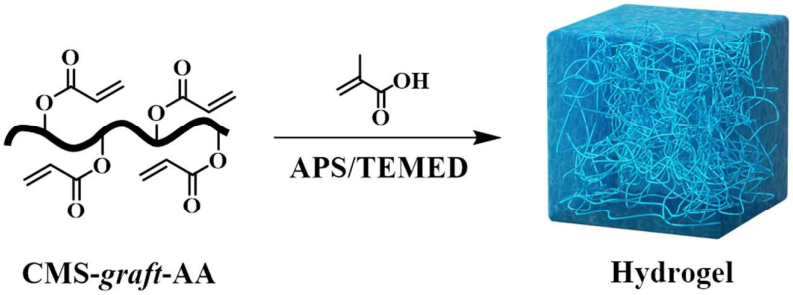

CMS-*graft*-AA **Hydrogel**

Scheme S1. (A) Chemical structure of CMS-*g*-AA. (B) Synthetic route for CMS-*g*-AA/PMAA hybrid hydrogel.

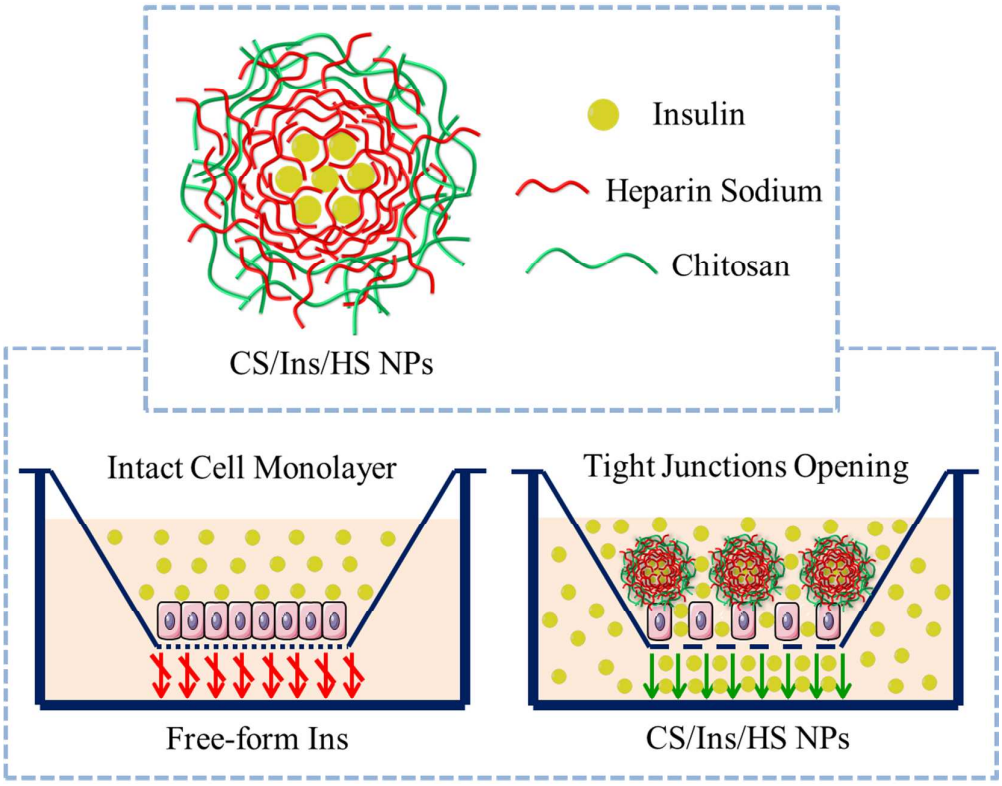

Scheme S2. Schematic illustrations for the compositions of CS/Ins/HS NPs and the enhancement of paracellular permeation of insulin (Ins) through the Caco-2 cell monolayer *via* the tight junctions (TJs) opening process.

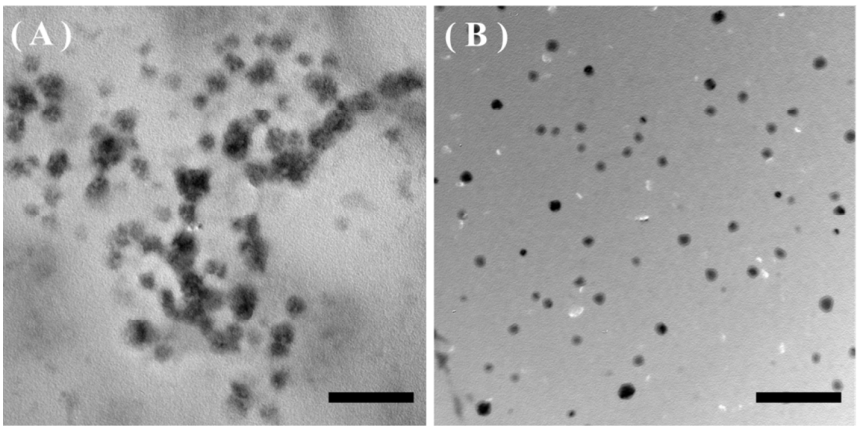

Figure S1. (A) Morphology of the Ins/HS aggregate in the feed ratio of 1/2 (wt/wt) between insulin (Ins) and heparin sodium (HS). (B) Morphology of the empty CS/HS nanoparticles in the feed ratio of 6/1 (wt/wt) between chitosan (CS) and heparin sodium (HS). The scale bar was 1 μm.

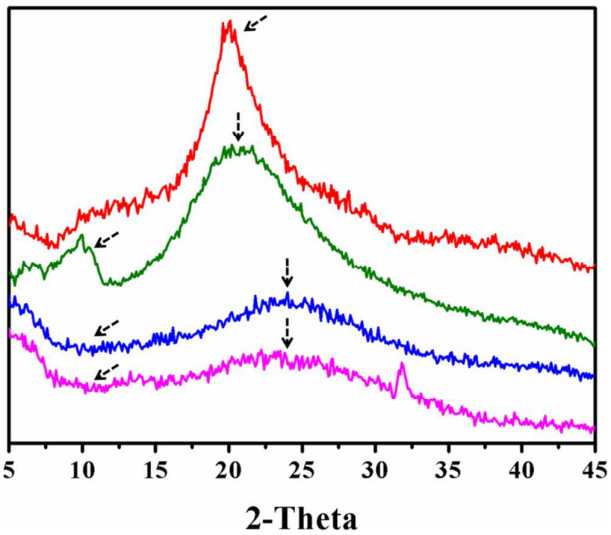

Figure S2. X-ray diffractograms of chitosan (CS, red line), insulin (Ins, green line), Ins/HS aggregates in Ins/HS feed ratio of 1/2 (wt/wt, blue line) and CS/Ins/HS NPs (pink line), arrayed in the turn from top trace to bottom trace.

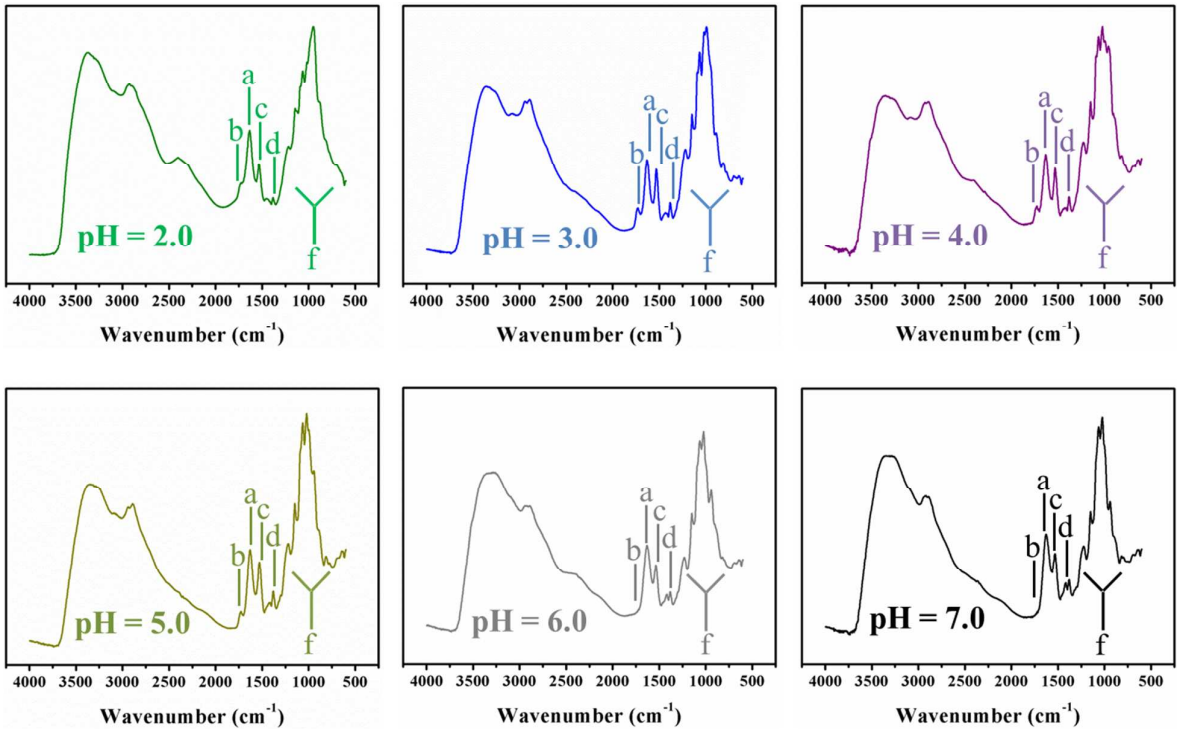

Figure S3. Reflective FT-IR spectra of the CS/Ins/HS NPs in different pH environments from pH 2.0 to pH 7.0 (I = 0.15 M).

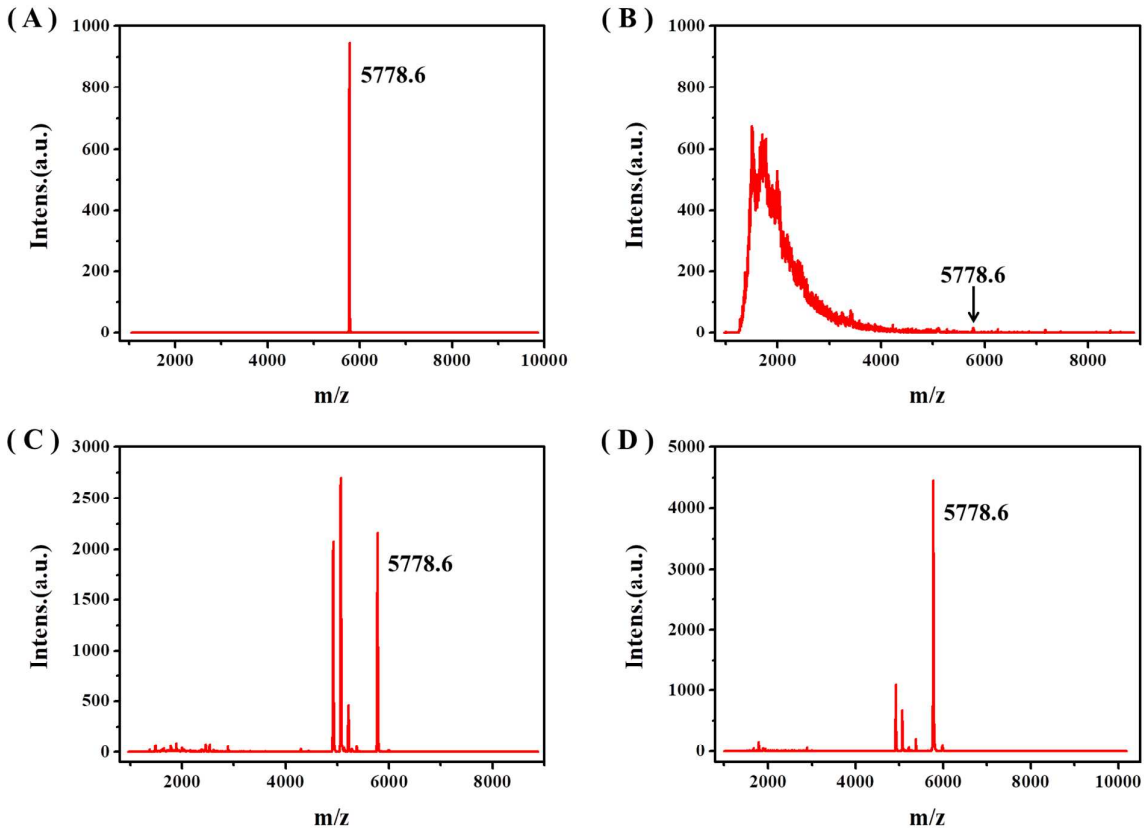

Figure S4. MALDI-TOF MS analysis for the insulin standard sample (A), the free-form insulin after incubating with trypsin (B), the insulin residue collected from the Ins/HS aggregates (Ins/HS feed ratio: 1/2, wt/wt) after incubating with trypsin (C), and the insulin residue collected from the CS/Ins/HS NPs after incubating with trypsin (D), respectively. The incubating time for each sample was set as 60 min.

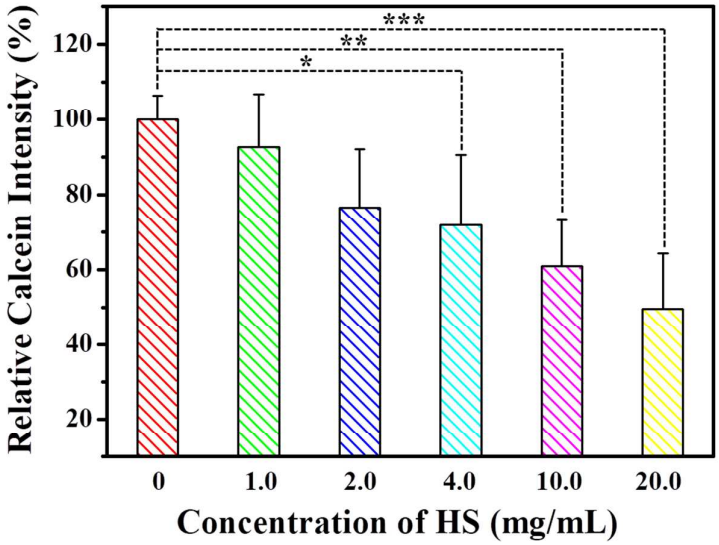

Figure S5. Fluorescent intensity of calcein-stained Ca^{2+} on Caco-2 cells after incubating with the heparin sodium (HS) solutions in different concentrations from 1.0 mg/mL to 20.0 mg/mL. The detection was carried out on a flow cytometer. The group treated with PBS (0 mg/mL of HS) was set as the negative control with 100% of the relative calcein intensity (n = 3, ***$p < 0.001$, **$p < 0.01$, *$p < 0.05$).

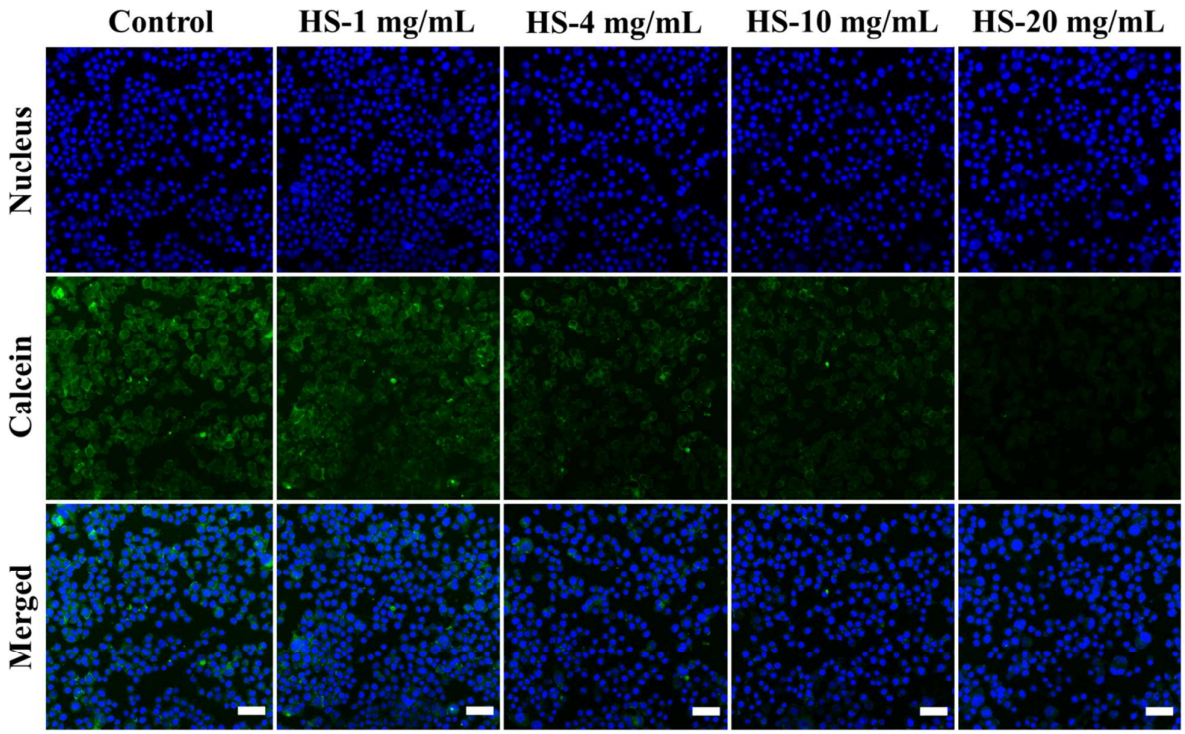

Figure S6. Confocal images showing the calcium levels on Caco-2 cells, as indicated by the green fluorecent intensity of calcein-stained Ca^{2+}, after incubating with the heparin sodium (HS) solutions in different concentrations from 1.0 mg/mL to 20.0 mg/mL. The cell nucleus was stained by 4'-6-diamidino-2-phenylindole (DAPI), and the calcium ions were stained by calcein. The group incubated with PBS was set as the control. Scale bar: 50 μm.

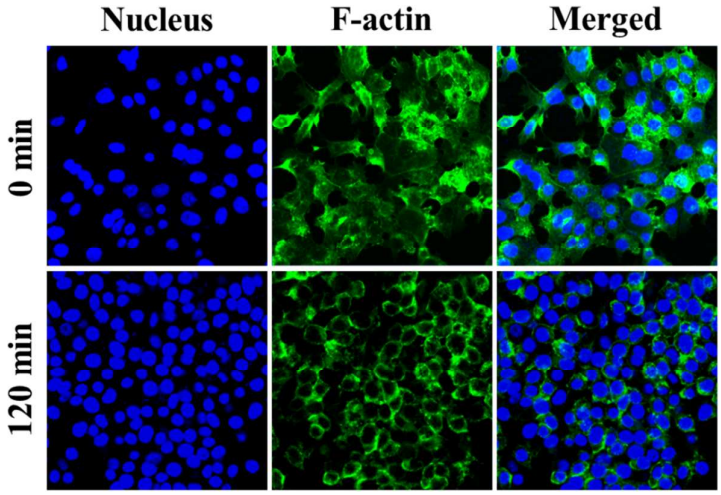

Figure S7. Visualization for the F-actin rearrangement in cytoskeleton of Caco-2 cells after incubating the cells with CS/Ins/HS NPs for 120 min. The morphology of the cells before incubation was presented as the control. The F-actin of Caco-2 cells was stained by Alexa Fluor 488 phalloidin (AF-488), while the cell nucleus was stained by DAPI. Scale bar: 50 μm.

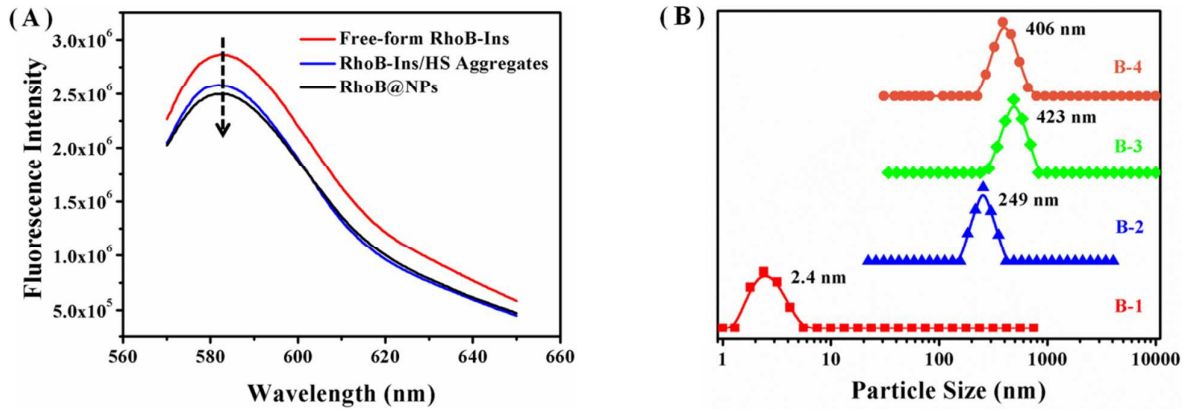

Figure S8. (A) Fluorescence curves for the solution of free-form RhoB-Ins solution (red line), the solution of RhoB-Ins/HS aggregates in the feed ratio of 1/2 (wt/wt, blue line), and the solution of RhoB@NPs (black line), respectively. The three solutions were all at pH 4.0, with the equal RhoB-Ins concentration of 0.1 mg/mL. (B) Particle size measurements for the free-form insulin (B-1), the Ins/HS aggragates in Ins/HS feed ratio of 1/2 (wt/wt, B-2), the CS/Ins/HS NPs (B-3) and the RhoB@NPs (B-4), respectively. The tests were performed at pH 4.0 with the specimen concentration of 0.2 mg/mL (I = 0.15 M).

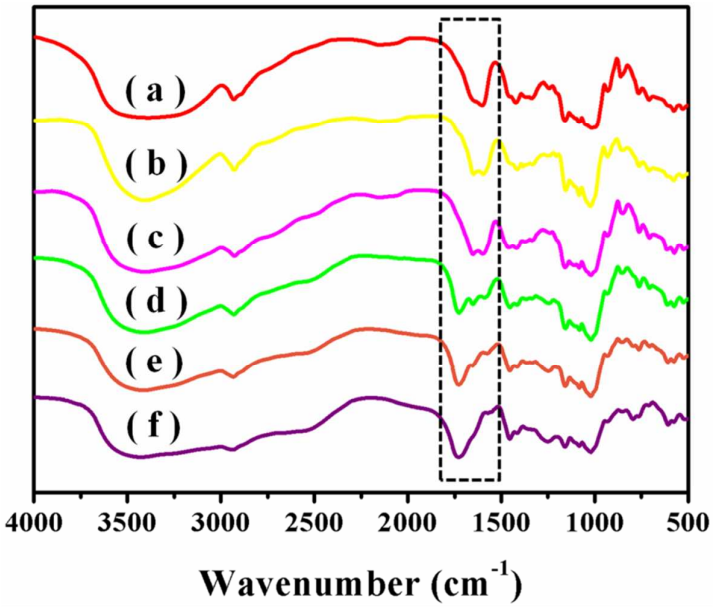

Figure S9. FT-IR spectra of CMS (a), CMS-*g*-AA (b), Gel-0 (c), Gel-1 (d), Gel-2 (e) and Gel-3 (f), respectively.

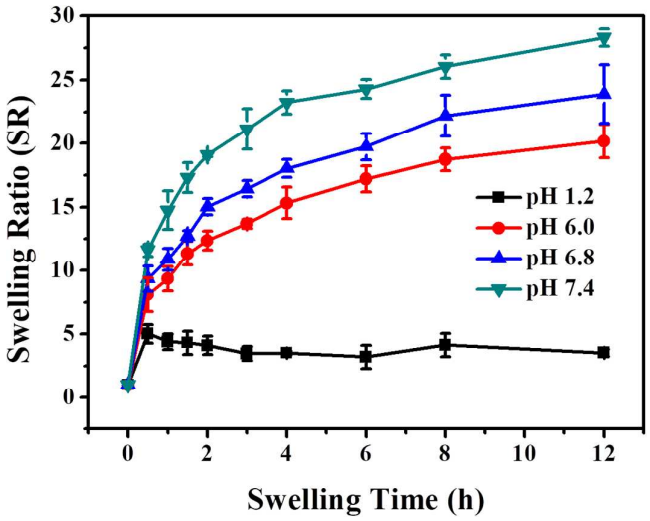

Figure S10. Swelling ratio (SR) *vs.* time curves of Gel-2 at different pH (n = 3).

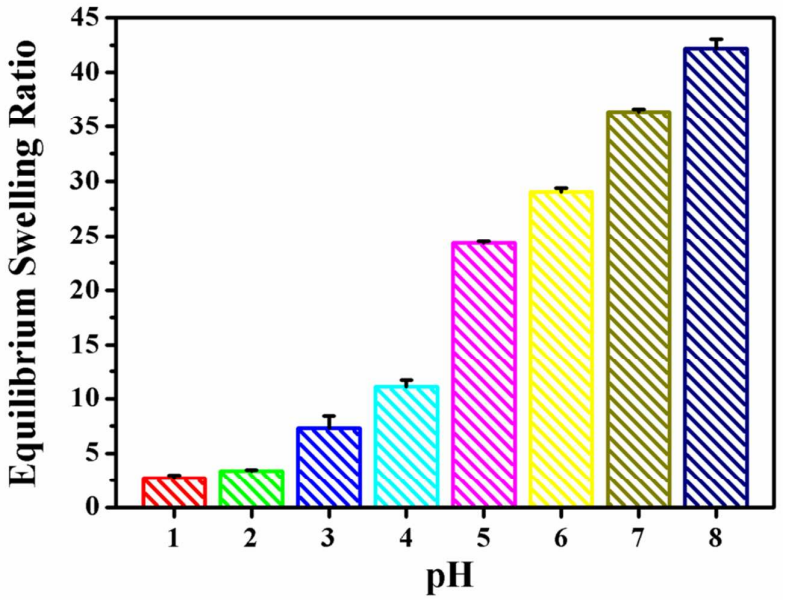

Figure S11. Equilibrium swelling ratios (ESRs) of Gel-2 at different pH from 1.0 to 8.0 (I = 0.15 M) (n = 3).

Figure S12. The image of Gel-2 after reaching the swelling equilibrium in AGF (pH 1.2, left) or in AIF (pH 6.8, right) (n = 3).

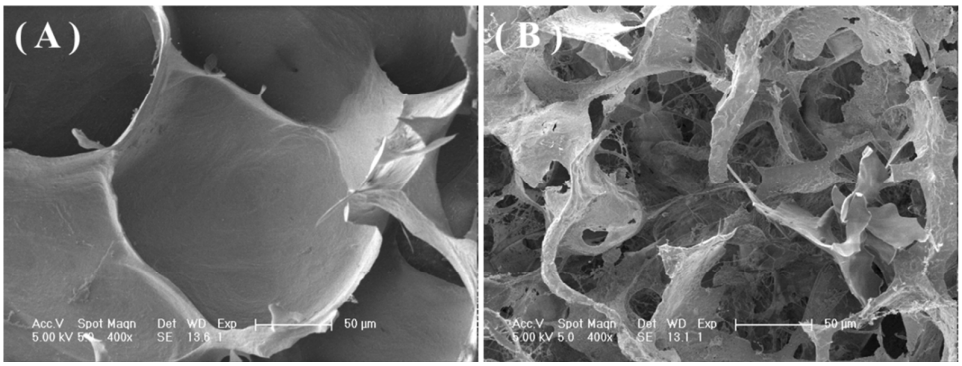

Figure S13. Morphology of Gel-2 after reaching the swelling equilibrium in AIF in absence of α-amylase (A) or after being incubated for 30 min in AIF in presence of α-amylase (B), as observed by the environmental scanning electron microscopy (ESEM). The concentration of α-amylase in AIF was set as 100 U/mL. The scale bar was 50 μm.

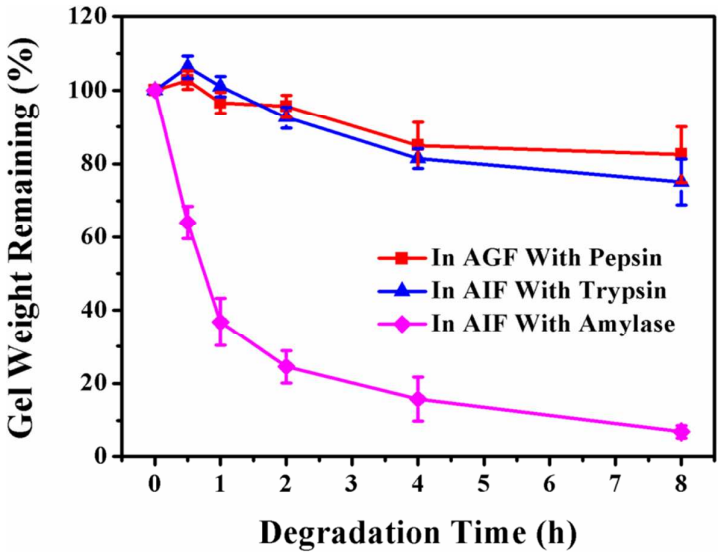

Figure S14. Degradation behaviors of Gel-2 after incubating in the media with different enzymatic environments. The media included the AGF containing pepsin (red line, 800 U/mL), the AIF containing trypsin (blue line, 3000 U/mL), and the AIF containing α-amylase (pink, 100 U/mL). The gel weight remaining (of initial %) *vs.* degradation time curves were presented (n = 3).

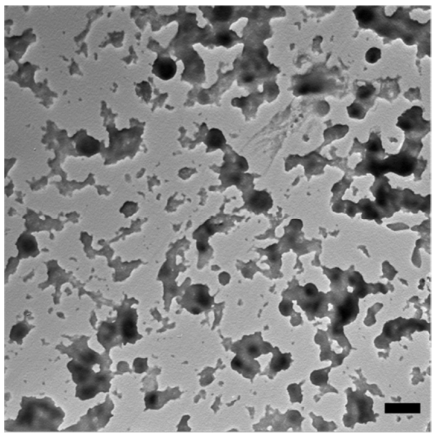

Figure S15. TEM image of the RhoB@NPs collected from the supernatant of RhoB@NPs@Gel-2 releasing system after incubating the RhoB@NPs@Gel-2 in AIF (containing α-amylase, 100 U/mL) for 60 min. The scale bar was 2 μm.